

New Reconstruction Technique for Echo-Planar Imaging to Allow Combined Use of Odd and Even Numbered Echoes

KENSUKE SEKIHARA AND HIDEKI KOHNO

Central Research Laboratory, Hitachi, Ltd., P.O. Box 2, Kokubunji, Tokyo 185, Japan

Received May 27, 1987; revised September 15, 1987

An image reconstruction technique for echo-planar imaging is proposed. This technique combines odd and even numbered echo signals. It is thus possible to reduce the frequency of the time-modulated gradient used in echo-planar imaging by 50%, and to reduce its amplitude by almost 50% for sinusoidal gradient modulation. © 1987 Academic Press, Inc.

INTRODUCTION

Up to now, various methods have been proposed for spatial mapping of a spin distribution using NMR. Several of these methods use field gradient time modulation for high-speed data acquisition. One such method is the well-known echo-planar imaging (1, 2). With this method, spin distributions can be imaged with a single spin-echo train induced by one 90° pulse application. However, the method imposes stringent requirements on the amplitudes and frequencies of the time-modulated gradient when the image matrix becomes large.

This paper proposes an image reconstruction technique that allows the combined use of odd and even numbered spin echoes. These echoes correspond to echoes induced by the positive and negative applications of the periodic gradient, respectively. With the proposed reconstruction technique, the amplitude and frequency of the time-modulated gradient can be reduced by up to 50% without sacrificing one-shot imaging capability.

METHOD

In echo-planar imaging with square-wave gradient modulation, the trajectory of data points in k space (spatial frequency domain) is expressed by a zig-zag line (3, 4), as shown in Fig. 1a. Here, it is assumed that the time-modulated gradient is applied in the x direction and the stationary gradient is applied in the y direction. k_x is the spatial frequency for the x direction and k_y is that for the y direction. Let us denote data arrays obtained from odd and even numbered echoes as $S_P(k_x, k_y)$ and $S_N(k_x, k_y)$, respectively. Note that the data points marked by (○) in Fig. 1a represent $S_P(k_x, k_y)$ and data points marked by (●) represent $S_N(k_x, k_y)$. Δk_y is the minimum distance of these data arrays in the k_y direction.

A cross section of the spatial frequency distribution at a specific k_x (indicated by the broken line in Fig. 1a) is shown in Fig. 1b. Sampling points within each of the two sets marked by (○) and (●) are equal intervals apart; the interval is equal to Δk_y .

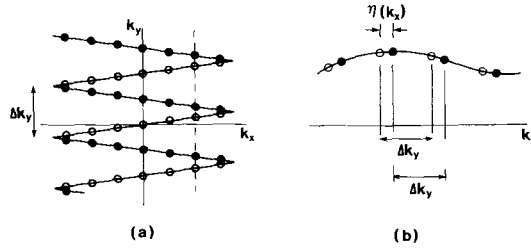


FIG. 1. (a) Typical k space trajectory for echo-planar imaging. Data points marked by (○) and (●) are obtained when the x gradient is positive and negative, respectively. (b) Cross section of spatial frequency distribution at a specific value of k_x (indicated by the broken line in (a)).

These sets of sampling points are separated by $\eta(k_x)$. In square-wave gradient modulation, $\eta(k_x)$ is given by

$$\eta(k_x) = \frac{\Delta k_y}{2} \left(1 - \frac{k_x}{k_x^{\max}} \right). \quad [1]$$

Here, k_x^{\max} is the maximum value of k_x in k space. The proposed technique can reconstruct images when Δk_y is set at twice the requirement from the sampling theorem, i.e., when Δk_y is set at $4\pi/L_y$, where L_y is the width of the field of view in the y direction.

Let us define $g_P(k_x, y)$ and $g_N(k_x, y)$ as the Fourier transforms of $S_P(k_x, k_y)$ and $S_N(k_x, k_y)$ with respect to k_y . $g_P(k_x, y)$ at a specific value of k_x is schematically depicted in Fig. 2a. As shown in this figure, $g_P(k_x, y)$ contains aliasing because Δk_y exceeds the requirement from the sampling theorem. However, applying the theory of interlaced sampling (5), one can remove aliasing by using $g_P(k_x, y)$ and $g_N(k_x, y)$. That is, to obtain an aliasing-free image, it is necessary to calculate

$$g(k_x, y) = \frac{-e^{\kappa 2\pi i \xi(k_x)}}{1 - e^{\kappa 2\pi i \xi(k_x)}} g_P(k_x, y) + \frac{e^{i y \eta(k_x)}}{1 - e^{\kappa 2\pi i \xi(k_x)}} g_N(k_x, y), \quad [2]$$

where $\xi(k_x) = \eta(k_x)/\Delta k_y$. In Eq. [2], $\kappa = -1$ for $y \geq 0$ and $+1$ for $y < 0$. $g(k_x, y)$ at the same k_x as that in Fig. 2a is shown in Fig. 2b.

Let us also calculate $h(k_x, y)$:

$$h(k_x, y) = \frac{1}{1 - e^{\kappa 2\pi i \xi(k_x)}} g_P(k_x, y) - \frac{e^{i y \eta(k_x)}}{1 - e^{\kappa 2\pi i \xi(k_x)}} g_N(k_x, y), \quad [3]$$

where $\kappa = -1$ for $y \geq 0$, and $+1$ for $y < 0$. Figure 2c shows $h(k_x, y)$ at the same k_x as that in Figs. 2a and 2b.

As suggested in Figs. 2b and 2c, an aliasing-free Fourier transform $G(k_x, y)$ can be obtained for $-L_y/2 \leq y \leq L_y/2$ through the following combination,

$$\begin{aligned} G(k_x, y) &= h\left(k_x, y + \frac{L_y}{2}\right) & -\frac{L_y}{2} \leq y < -\frac{L_y}{4}, \\ G(k_x, y) &= g(k_x, y) & -\frac{L_y}{4} \leq y \leq \frac{L_y}{4}, \\ G(k_x, y) &= h\left(k_x, y - \frac{L_y}{2}\right) & \frac{L_y}{4} < y \leq \frac{L_y}{2}. \end{aligned} \quad [4]$$

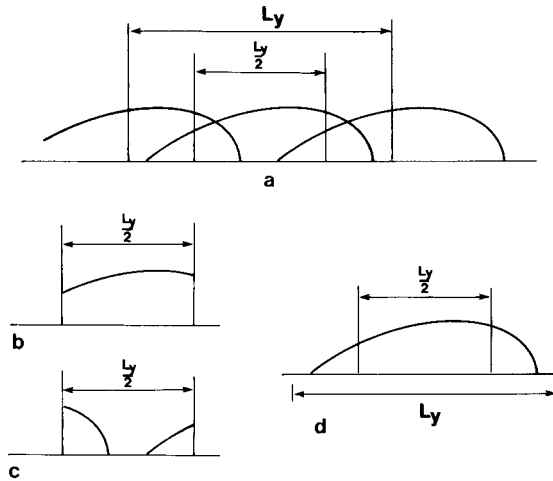


FIG. 2. (a) $g_p(k_x, y)$ at a specific k_x . (b) $g(k_x, y)$ at same k_x as in (a). (c) $h(k_x, y)$ at same k_x as in (a). (d) $G(k_x, y)$ at same k_x as in (a), (b), and (c).

$G(k_x, y)$ at the same k_x as that in Figs. 2a–2c is shown in Fig. 2d. The final image can be reconstructed by Fourier transforming $G(k_x, y)$ with respect to k_x .

This technique can be applied to echo-planar imaging using sinusoidal gradient modulation with no modification except using

$$\eta(k_x) = \frac{\Delta k_y}{2} \left[1 - \frac{2}{\pi} \arcsin \left(\frac{k_x}{k_x^{\max}} \right) \right], \quad [5]$$

instead of using Eq. [1].

COMPUTER SIMULATION

Computer simulation has been performed to demonstrate the effectiveness of this method. The phantom pattern generated in computer simulation is shown in Fig. 3. Assuming square-wave modulation, one calculates $S_p(k_x, k_y)$ and $S_N(k_x, k_y)$ with 128 discrete k_x values and 64 discrete k_y values. Here, Δk_y was set at $4\pi/L_y$, twice the

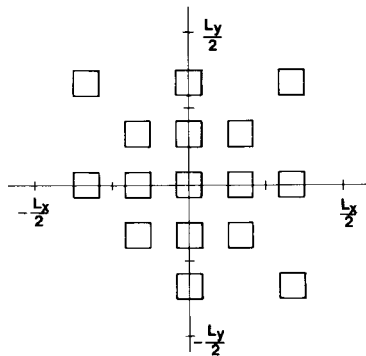


FIG. 3. Phantom pattern generated in computer simulation.

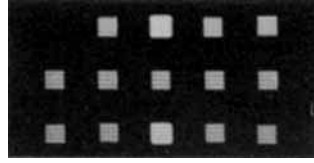


FIG. 4. Image obtained by Fourier transforming $S_P(k_x, k_y)$ with respect to k_x and k_y . Image consists of 128×64 pixels.

requirement from the sampling theorem. The image obtained through two-dimensional Fourier transform of $S_P(k_x, k_y)$ with respect to k_x and k_y is shown in Fig. 4. This image consists of 128×64 pixels. The image contains aliasing because Δk_y does not satisfy the sampling theorem's requirement.

Figure 5a shows the image obtained by Fourier transforming $g(k_x, y)$ with respect to k_x . The image obtained from $h(k_x, y)$ is shown in Fig. 5b. These figures indicate that the technique presented here makes it possible to separate the image from its overlapped replicas. The Fourier transform of $G(k_x, y)$ with respect to k_x is shown in Fig. 6. This image consists of 128×128 pixels. This figure clearly shows that the image free from aliasing can be obtained with this technique.

NOISE INCREASE AND AMPLITUDE REDUCTION OF MODULATED GRADIENT

One drawback in the proposed reconstruction technique is an increase in noise in the final reconstructed image. This noise increase is caused by the complex weighting factor, $1/\{1 - \exp[\kappa 2\pi i \xi(k_x)]\}$, contained on the right-hand sides of Eqs. [2] and [3].

Let us define the absolute values of the weighting factor as $W(k_x)$, i.e., $W(k_x) = 1/|1 - \exp[\kappa 2\pi i \xi(k_x)]|$. $W(k_x)$ is shown as a function of k_x/k_x^{\max} in Fig. 7. $W(k_x)$ is less than 1 when $k_x/k_x^{\max} < 0.7$ for square-wave modulation. It is also less than 1 when $k_x/k_x^{\max} < 0.85$ for sinusoidal modulation. Thus, noise increase in an image can be avoided by reconstructing the image using only the data with k_x less than Γk_x . Γ is, for example, 0.7 for square-wave modulation and 0.85 for sinusoidal modulation.

Noise increase as a function of Γ can be more accurately estimated as follows. The noise rms of an image reconstructed using the conventional method is denoted as σ_0 . In conventional reconstruction, $g_P(k_x, y)$ and $g_N(-k_x, y)$ are separately Fourier transformed with respect to k_x , and added to produce the final image. The noise rms values of $g_P(k_x, y)$ and $g_N(k_x, y)$ are assumed to be equal and are denoted as σ_C . It is also assumed that the noise contained in $g_P(k_x, y)$ has no correlation with that contained in $g_N(k_x, y)$. Thus, σ_0 can be calculated from

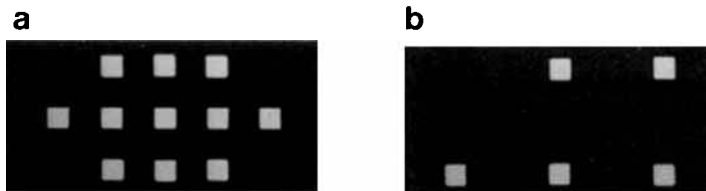


FIG. 5. (a) Image obtained by Fourier transforming $g(k_x, y)$ with respect to k_x . (b) Image obtained by Fourier transforming $h(k_x, y)$ with respect to k_x .

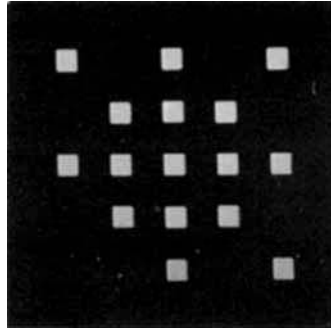


FIG. 6. Image obtained by Fourier transforming $G(k_x, y)$ with respect to k_x . Image consists of 128×128 pixels.

$$\sigma_0^2 = 2 \int_{-k_x^{\max}}^{k_x^{\max}} \sigma_c^2 dk_x = 4k_x^{\max} \sigma_c^2. \tag{6}$$

The amplitude of the periodic gradient used in conventional image reconstruction is denoted as G_x^C , and the gradient period as $4T_w$. With γ defined as the gyromagnetic ratio, k_x^{\max} is equal to $\gamma G_x^C T_w$ in this case.

The rms value of the noise contained in $G(k_x, y)$ is denoted as σ_G . The noise rms values for $g_P(k_x, y)$ and $g_N(k_x, y)$ are denoted as σ_D . Then, the equation $\sigma_G^2 = 2W^2(k_x)\sigma_D^2$ is derived using Eqs. [2] and [3]. First square-wave gradient modulation is considered. When the data between $-\Gamma k_x^{\max}$ and Γk_x^{\max} are used for image reconstruction, the noise rms, σ , of the final image reconstructed with the proposed technique is given by

$$\sigma^2 = \sigma_D^2 \int_{-\Gamma k_x^{\max}}^{\Gamma k_x^{\max}} 2W^2(k_x) dk_x = \frac{\sigma_D^2 k_x^{\max}}{\pi} \left\{ \cot \left[\frac{\pi}{2} (1 - \Gamma) \right] - \cot \left[\frac{\pi}{2} (1 + \Gamma) \right] \right\}. \tag{7}$$

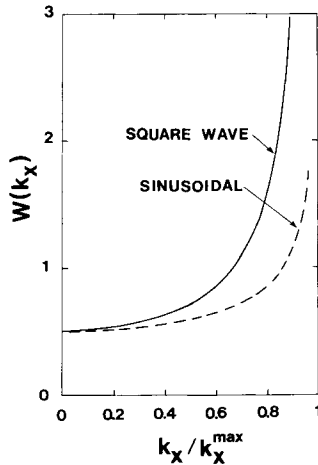
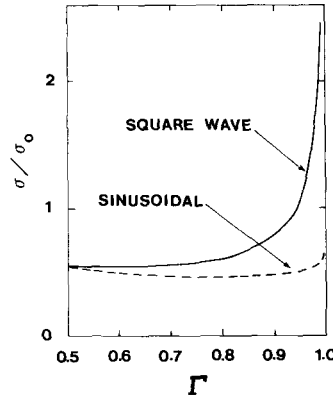


FIG. 7. Absolute values of the complex weighting factor, $W(k_x)$, as a function of k_x/k_x^{\max} .

FIG. 8. Noise increase σ/σ_0 as a function of Γ .

Since the amplitude of the periodic gradient is denoted as G_x^D in this case, k_x^{\max} is equal to $\gamma G_x^D(2T_w)$. Here, the period of the x gradient must be set at $8T_w$. Therefore, we can finally obtain from Eqs. [6] and [7]

$$\frac{\sigma}{\sigma_0} = \frac{1}{2\Gamma} \sqrt{\frac{1}{2\pi} \left\{ \cot \left[\frac{\pi}{2} (1 - \Gamma) \right] - \cot \left[\frac{\pi}{2} (1 + \Gamma) \right] \right\}}. \quad [8]$$

In deriving Eq. [8], it is assumed that $\gamma G_x^C T_w = \Gamma \gamma G_x^D(2T_w)$, and $(\sigma_C/\sigma_D)^2 = G_x^C/G_x^D = 2\Gamma$. For sinusoidal gradient modulation, using Eq. [5], we can derive

$$\frac{\sigma}{\sigma_0} = \frac{1}{2\Gamma} \sqrt{\frac{1}{4} \log \left| \tan \left\{ \frac{\pi}{4} \left[1 + \frac{2}{\pi} \arcsin(\Gamma) \right] \right\} - \tan \left\{ \frac{\pi}{4} \left[1 - \frac{2}{\pi} \arcsin(\Gamma) \right] \right\} \right|}. \quad [9]$$

Noise increase caused by the proposed reconstruction technique can be evaluated using Eqs. [8] and [9]. The calculated results of σ/σ_0 as a function of Γ are shown in Fig. 8. This figure indicates that when Γ is less than 0.95, the ratio σ/σ_0 is less than 1 for square-wave modulation. Noise increase is shown to be almost negligible for sinusoidal modulation except when $\Gamma = 1$.

Since only the data between $-\Gamma k_x^{\max}$ and Γk_x^{\max} are used for image reconstruction, the amplitude of the x gradient must be increased by $1/\Gamma$ to maintain the same spatial resolution. Accordingly, the proposed reconstruction cannot reduce the periodic gradient amplitude to exactly 50% of that required for conventional reconstruction. This amplitude reduction of the periodic gradient attained by the proposed reconstruction technique can be evaluated by $G_x^D/G_x^C = 1/(2\Gamma)$. Thus, it is concluded that the proposed reconstruction can reduce the periodic gradient amplitude required for conventional reconstruction to 53% for square-wave modulation without increasing image noise, and to almost 50% for sinusoidal modulation.

CONCLUSIONS

A new image reconstruction technique for echo-planar imaging has been proposed. This technique permits reducing the frequency of the time-modulated gradient by

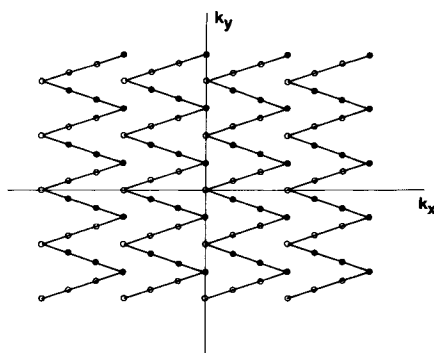


FIG. 9. An example of k trajectories for data obtained by fast Fourier imaging. Four trajectories are combined in this example. Data points marked by (○) and (●) are obtained when the x gradient is positive and negative, respectively.

50%. Analysis of the noise caused by this technique shows that the amplitude of the time-modulated gradient can also be reduced by approximately 53% for square-wave modulation and by almost 50% for sinusoidal modulation, without increasing noise in the reconstructed image.

The k trajectories of data measured by fast Fourier imaging proposed by Van Uijen *et al.* (6) are shown in Fig. 9. Multiple trajectories are combined to reconstruct an image by this method. It is clear in this figure that the proposed technique is applicable to this imaging method. In this imaging method, the speed-up factor q is defined as $q = M/N$, where N is the number of measurements needed for image formation, and M is the size of the image matrix. It is easy to show that the proposed technique can nearly double the speed-up factor without increasing image noise.

Finally, high-speed spectroscopic imaging by gradient time modulation has recently been proposed (7, 8). The modulation frequency limits the spectral bandwidth in this spectroscopic imaging. Thus, stringent requirements are also imposed on gradient modulation if the method is applied to nuclei with large chemical-shift dispersions, such as ^{31}P , at higher field strengths. The reconstruction technique presented in this paper is also applicable to such spectroscopic imaging.

ACKNOWLEDGMENTS

The authors thank Dr. S. Matsui and Mr. T. Onodera for their helpful discussions.

REFERENCES

1. P. MANSFIELD, *J. Phys. C*, **10**, L55 (1977).
2. P. MANSFIELD AND I. L. PYKETT, *J. Magn. Reson.* **29**, 355 (1978).
3. D. B. TWIEG, *Med. Phys.* **10**, 610 (1983).
4. S. LJUNGGREN, *J. Magn. Reson.* **54**, 338 (1983).
5. R. N. BRACEWELL, "Fourier Transform and its Applications," McGraw-Hill, New York, 1978.
6. C. M. J. VAN UIJEN, J. H. DEN BOEF, AND F. J. J. VERSCHUREN, *Magn. Reson. Med.* **2**, 203 (1985).
7. P. MANSFIELD, *Magn. Reson. Med.* **1**, 370 (1984).
8. S. MATSUI, K. SEKIHARA, AND H. KOHNO, *J. Magn. Reson.* **67**, 476 (1986).